

Ethanollic Extract of Cockroach Wing Powder as Corrosion Inhibitor for N80 Steel in an ASTM D1141-98(2013) Standard Artificial Seawater Solution

Shivani Singh¹, Rahul Singh^{1,*}, Neeta Raj Sharma^{1,*}, Ambrish Singh^{2,*}

¹ School of Bioengineering and Biosciences, Lovely Professional University, Phagwara, Punjab, India-144402.

² School of New Energy and Materials, Southwest Petroleum University, Chengdu-610500, Sichuan, China.

*E-mail: neeta.raj@lpu.co.in; rahul.16188@lpu.co.in; vishisingh4uall@gmail.com

Received: 6 May 2021 / Accepted: 4 June 2021 / Published: 30 June 2021

Electrochemical, localized electrochemical and surface exploration procedures were used to investigate the potential of wings plucked from adult cockroaches (WAC) to attenuate N80 steel corrosion in simulated saltwater. According to the impedance studies, a maximum inhibition efficacy of 96.8% was recorded with 400 mg/L of WAC inhibitor in corrosive environments. This was owing to the steel's increased resistance as the compounds from WAC extract effectively occluded the corrosion centers. With 94 percent efficiency in the corrosive solution, electrochemical frequency modulation (EFM), a novel and prominent technology, also revealed that WAC has high mitigation ability. On the N80 steel, the polarization data revealed a cathodic preponderance of WAC inhibitor. To control localized corrosion, researchers used scanning electrochemical microscopy (SECM) and scanning Kelvin probe (SKP) techniques. The WAC film development is shown using scanning electron microscopy (SEM).

Keywords: N80 steel; Cockroach wings; Corrosion; SKP

1. INTRODUCTION

Corrosion may be seen in all metallic components across the planet. All engineering systems, whether in clean energy, water delivery, shipping, food, the business sector, management plants, boilers, and storage reservoirs, are susceptible to corrosion, resulting in their deterioration. Stents in the heart, wires in the teeth, Mg/Ti implants in the body, and nuclear power plants are all examples of corrosion. Corrosion is a trendy issue of study for new scientists and students who are putting themselves in the shoes of current academics and famous scientists to discover a suitable solution [1-5] because of its prevalence in industries and diverse domains.

Corrosion is a major concern across the world, costing billions of dollars each year. This economic disaster must be averted with the use of appropriate and modern approaches. Despite the fact that scientists and writers have developed new approaches based on ceramics, polymers, glass, and other materials that are compatible with the old ones. Even yet, there is a constant need for low-cost corrosion inhibitors that comply with environmental requirements. To generate low-cost potential inhibitors, plant extracts, natural goods, waste goods, and recycled goods are being employed. The experiments of cockroach wings as a possible corrosion inhibitor were undertaken with legislation and waste management in mind [6-10].

Cockroaches have been observed in nuclear testing reactors and are known to thrive in extreme temperatures and pressure. They may live in these circumstances by using their wings to cover their bodies under them. After the dissection tests were completed, the dead cockroaches were gathered from several institutions in Varanasi, Uttar Pradesh, India. Several studies were carried out to demonstrate their efficacy as a N80 steel inhibitor in artificial seawater medium.

2. EXPERIMENTAL PROCEDURES

2.1. Inhibitor

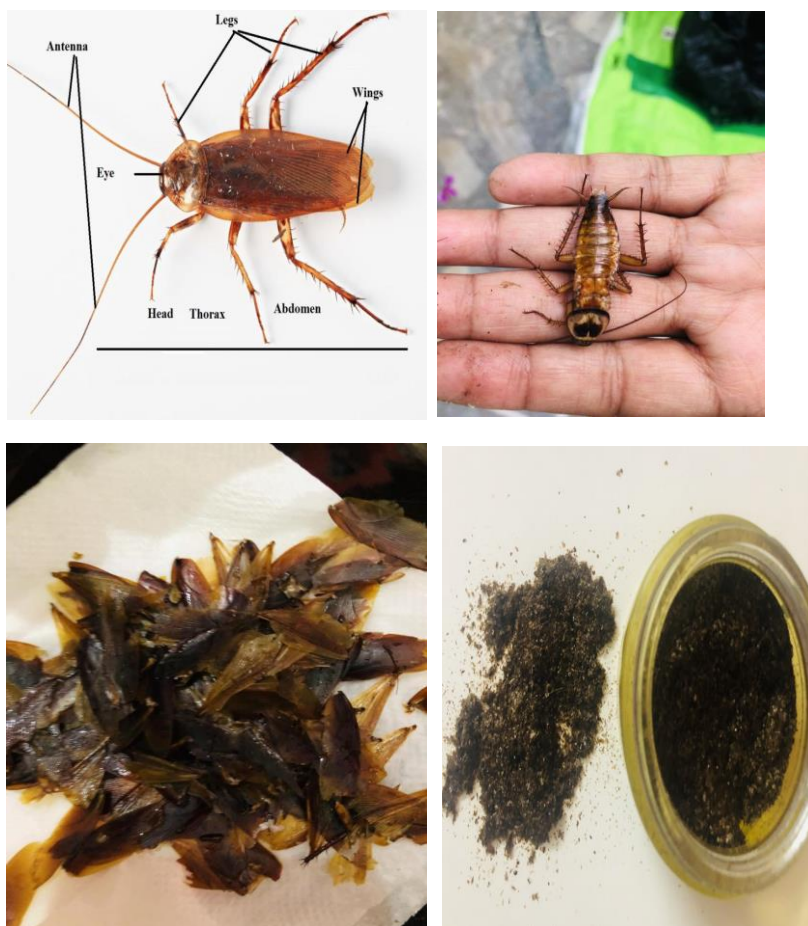


Figure 1 .(a) Various body parts of the Cockroach, (b) Cockroach without wings, (c) wings plucked from the dead cockroaches, and (d) powdered wings.

As illustrated in Fig. 1, adult cockroaches were gathered from several institutions in Varanasi, Uttar Pradesh, India. The wings were carefully picked from the dead cockroaches and dried for 5 days in the sun. The wings were subjected to a mixer grinder while they dried adequately. The dried wings were ground into a powder, which was combined with ethanol and stored in a Soxhlet column for extraction. The extracted solution was concentrated using an artificial saltwater solution before being employed in corrosion testing.

2.2. Materials

Copper wire was welded to one end of the N80 steel electrode, which was then coated with epoxy resin. Before each experiment, a 1cm² area was abraded with silicon sheets of various pore sizes. In an ultrasonic tank, the electrode was extensively cleaned with water, acetone, and lastly ethyl alcohol. The steel electrode was vacuum dried to guarantee that it had no water on it. The artificial saltwater corrosive solution was prepared according to ASTM D1141-98 (2013) standard [11]. The chemical components of the artificial saltwater are shown in Table 1. The artificial seawater's pH was discovered to be 8.2 by using a digital pH meter.

Table 1. Chemical composition of ASTM standard D1141-98(2013) artificial seawater.

Compound	NaCl	MgCl ₂	Na ₂ SO ₄	NaHCO ₃	H ₃ BO ₃	CaCl ₂	KCl	SrCl ₂	KBr	NaF
C (g /dm ³)	24.5	5.20	4.09	0.201	0.027	1.16	0.69	0.025	0.101	0.003

2.3. Electrochemical Research

Gamry digital setup with three electrode assembly was used to perform impedance, frequency modulation, and polarization methods. The conventional electrochemical setup includes a reference electrode of Ag/AgCl, a counter electrode of graphite, and a working electrode of N80 [12]. Before starting each test, the setup was allowed for an hour to obtain a steady potential. Each test was carried out three times, and the results are shown with the standard deviations. Using the formulae below, the inhibition efficiency from impedance and polarization tests was calculated:

$$\eta_{EIS} = \frac{R_{(inh)} - R}{R_{(inh)}} \times 100 \quad (1)$$

$$\eta_{PDP} = \frac{i_{corr} - i_{corr(inh)}}{i_{corr}} \times 100 \quad (2)$$

where $R_{(inh)}$ is the charge transfer resistance of WAC inhibitor and R is the charge transfer resistance of artificial seawater, respectively. The current density of artificial seawater is represented by i_{corr} , while the current density of WAC inhibitor is represented by $i_{corr(inh)}$ [13].

Electrochemical frequency modulation (EFM) studies used frequencies of 2 and 5 Hz with 10 mV amplitude [14]. The Princeton workstation was used to perform scanning electrochemical microscopy (SECM) and scanning Kelvin Probe (SKP) tests. The silver Pt/Ir probe had a diameter of 10 mm and vibrated with 30 mm amplitude across the steel surface [15].

2.4. Surface analyses

To undertake Scanning electron microscopy (SEM) experiments, the surface of N80 steel was exposed to the ZiessEvo 50 XVP instrument before and after immersion in the simulated saltwater medium.

3. RESULTS AND DISCUSSION

3.1. Electrochemical analyses

3.1.1. Electrochemical impedance spectroscopy (EIS)

Impedance experiments were carried out in artificial seawater medium with various doses of WAC inhibitor to determine the maximal charge transfer resistance in comparison to a blank (artificial seawater media without inhibitor). Nyquist (Fig. 2a), Bode (Fig. 2b), and Phase angle (Fig. 2c) graphs are used to represent the impedance findings. When the x and y axes have the same value, the low semicircle may be observed in the medium frequency zone. The presence of an inductive groove in the lower frequency zone is typically ascribed to surface roughness. Because the corrosion process was comparable, all of the Nyquist plots in the aggressive medium had the same shape [16]. The charge transfer resistance (R_{ct}) is shown by the diameter of the Nyquist plots, which rose as WAC concentration rose. This is due to WAC inhibitor's ability to effectively mitigate steel corrosion in simulated saltwater [17, 18].

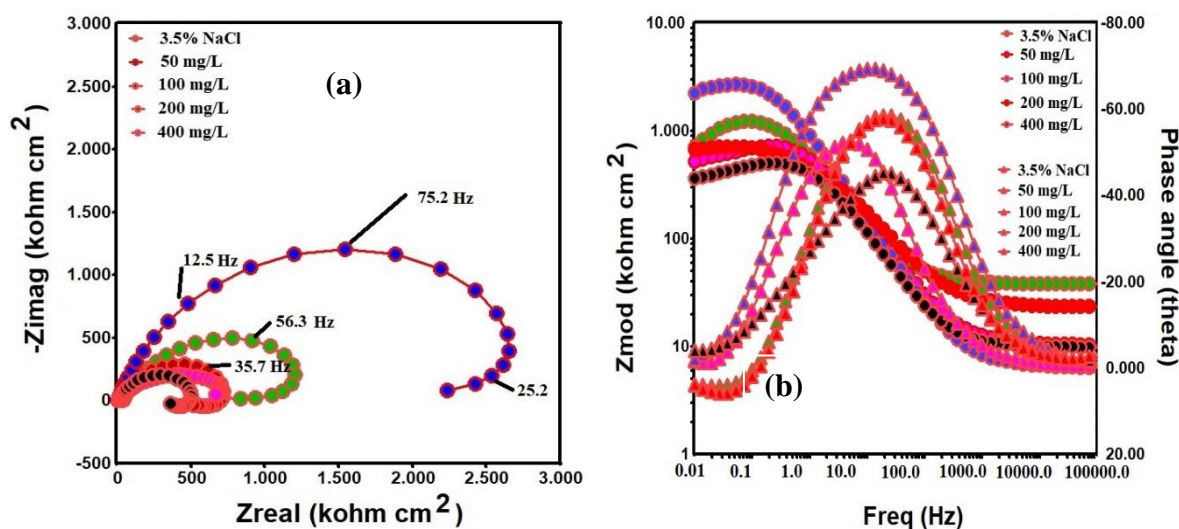


Figure 2. (a)Nyquist plot of WAC in artificial seawater solution and (b)Bode and phase angle plots for N80 steel in artificial seawater solution at 10 mV amplitude.

The slope values (-S) of the Bode graphs (Fig. 2b) tend to shift towards 1 when the concentration of WAC inhibitor increases. The phase angle (α°) graphs (Fig. 2b) showed a similar pattern, with peak values increasing towards 80°. For N80 steel in corrosive solution, the greatest slope

value of 0.82 and the greatest peak of 68.7° were achieved at 400 mg/L WAC concentration. The rise in steel resistance is responsible for these variations in values and the propensity to approach maximum. The compounds from WAC extract that create a protective layer on the steel surface are responsible for the increased resistance [19].

Compounds from WAC extract adsorb on the N80 steel surface, causing the effect. The acquired data was evaluated using the Echem analyzer software's related model (Fig. 3), and the findings are reported in Table 2. The model fits the graph extremely well, and the standard deviation is lower after three repeated tests, indicating that the model is well-fitting.

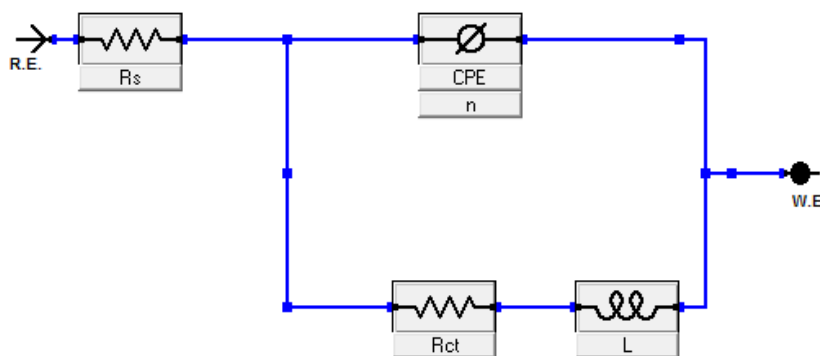


Figure 3. Equivalent circuit used to fit the Nyquist plots.

A double layer capacitance constant phase element (CPE), a charge transfer resistance (R_{ct}), a solution resistance (R_s), and an inductance make up the model (L). To acquire a good match and exact matching values, CPE was previously utilized in lieu of pure capacitor. The CPE impedance was calculated using the following equation (ZCPE):

$$Z_{CPE} = Y_0 [j\omega^\alpha]^{-1} \quad (3)$$

Where j be the complex value ($j = \sqrt{-1}$), Y_0 be the admittance and invariant for CPE, ω be the angular frequency in rad/s and α , be the phase shift [20]. The Compounds from WAC extract increase the resistance and affect the property of pure capacitor through adsorption on the steel/solution intersection.

Table 2 demonstrates that when the R_{ct} value increases, the WAC inhibitor's inhibitory effectiveness in an artificial seawater medium increases as well. According to the fit result, the value of inductance (L) is likewise tabulated. Inductance (L) is included in the circuit as it fits the inductive loop at the lower frequency zone in the Nyquist graph. Due to changes in the homogeneity of the solution as well as changes at the metal/solution interface, the values of phase change (n) tend to shift towards unity. This behavior is linked to the surface absorption of compounds from WAC extract on N80 steel, which reduces corrosive media penetration [21].

Table 2. Electrochemical impedance parameters of N80 steel in artificial seawater solution with standard deviation (\pm SD) at different concentration of the inhibitor.

C_{inh} (mg/L)	R_s (Ωcm^2)	R_{ct} ($\Omega\text{ cm}^2$)	$Y0^*$ ($\Omega^{-1}\text{s}^n/\text{cm}^2$)	n	L (H cm^2)	-S	α ($^\circ$)	η_{EIS} (%)
Blank	1.7	406.9 \pm 0.018	126.4	0.452	56.7	0.34	41.4	--
50	0.28	510.2 \pm 0.014	89.87	0.684	47.7	0.55	45.2	86.2
100	0.46	581.8 \pm 0.019	97.43	0.729	22.6	0.68	57.1	87.9
200	1.04	914.4 \pm 0.121	57.70	0.776	35.4	0.73	57.9	90.3
400	0.77	2332.2 \pm 0.229	116.1	0.808	10.1	0.82	68.7	96.8

EFM is a good approach for determining corrosion rate and efficiency in a short amount of time without prior knowledge of Tafel constants [22]. Figure 4 shows the frequency and intermodulation spectra acquired from EFM experiments.

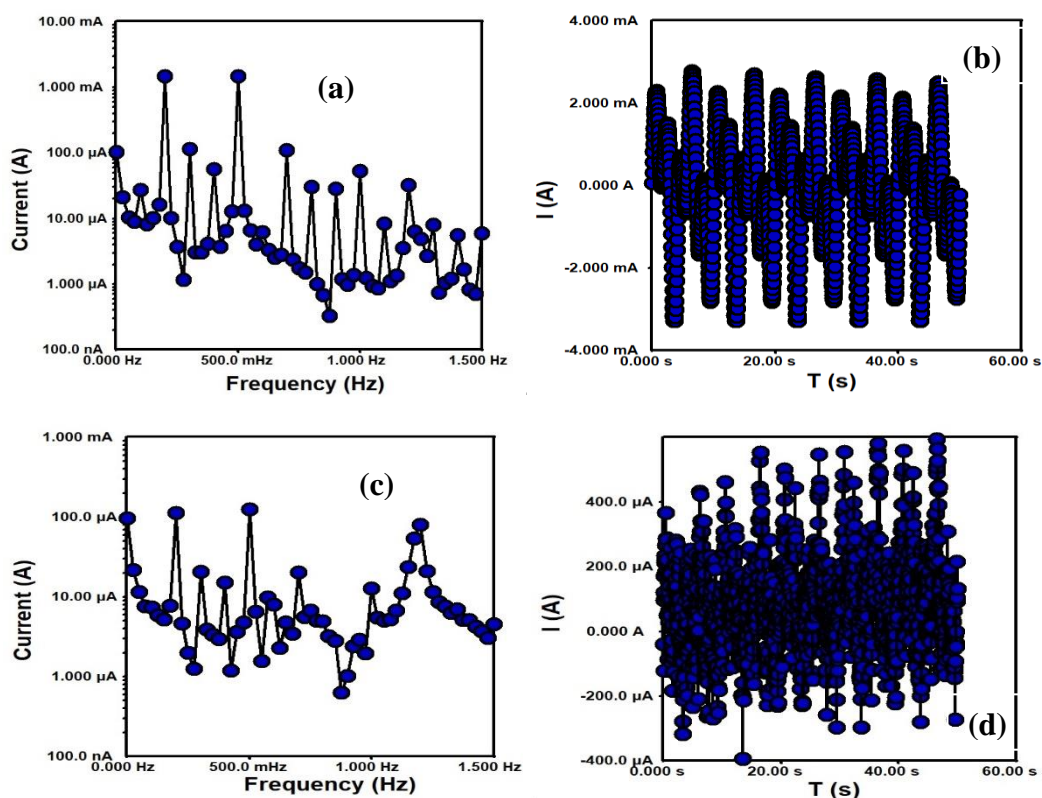


Figure 4. (a) Electrochemical frequency modulation curves for Blank + N80 steel and (b) Intermodulation curves for Blank + N80 steel (c) Electrochemical frequency modulation curves for inhibitor + N80 steel and (d) Intermodulation curves for inhibitor + N80 steel.

The assessed values of the investigated inhibitor in artificial seawater medium are shown in Table 3. The corrosive media's corrosion current density (i_{corr}) is larger, whereas the WAC inhibited solution's is lower. Table 3 shows that the casualty factors 2 and 3 are in agreement with and perfectly

comparable to the hypothetical variables of the published EFM idea [23]. The equation below was used to calculate the inhibition efficiency ($\eta_{EFM}\%$) using the i_{corr} values.

$$\eta_{EFM} \% = \left(1 - \frac{i_{corr}^{inh}}{i_{corr}^{blank}} \right) \times 100 \tag{11}$$

where i_{corr}^{blank} and i_{corr}^{inh} be the corrosion current densities in the absence and presence of the studied inhibitor, respectively. The inhibition efficiency of 94% was exhibited by the WAC inhibitor at 400 mg/L concentration.

Table 3. Electrochemical frequency modulation parameters for N80 steel in artificial seawater solution.

Solution	i_{corr}	β_a	$-\beta_c$	CF-2	CF-3	η_{EFM}
	($\mu\text{A}/\text{cm}^2$)	(mV/dec)	(mV/dec)			(%)
Blank	997.6	104	165	1.991	2.986	--
WAC	62.7	57	93	2.006	3.107	94.0

3.1.2. Potentiodynamic polarization (PDP)

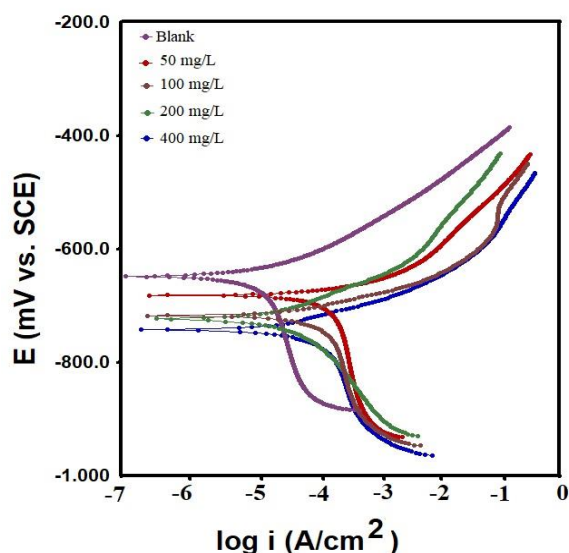


Figure 5. Potentiodynamic polarization curves for N80 steel in artificial seawater solution at 1 mV/s.

To acquire the PDP curves, polarization experiments were done using artificial seawater in the absence and presence of WAC inhibitor (Fig. 5). Table 4 shows the values of several parameters extrapolated from the graph. As can be seen in the table, i_{corr} values tend to drop as the amount of

WAC inhibitor increases. This behavior is linked to the adsorption of Compounds from WAC extract on the steel surface, which prevents artificial seawater from penetrating the active corrosion sites.

Table 4. Potentiodynamic polarization parameters of N80 steel in artificial seawater solution with stander deviation (\pm SD) at different concentration of the inhibitor at 1 mV/s.

Inhibitor (mg/L)	E_{corr} (V/SCE)	i_{corr} (A/cm²)	β_a (mV/dec)	$-\beta_c$ (mV/dec)	η_{PDP} (%)
Blank	-0.681	2.21 \pm 0.038	42	53	--
50	-0.717	0.77 \pm 0.033	57	76	65.0
100	-0.724	0.53 \pm 0.008	61	83	76.0
200	-0.743	0.13 \pm 0.033	78	64	94.0
400	-0.761	0.09 \pm 0.016	32	103	96.0

Despite the fact that both the cathodic and anodic sections have been changed, a significant cathodic dominance can be seen. In contrast to artificial seawater, the E_{corr} readings for WAC exhibit differences within 80 mV. In the aggressive medium, WAC inhibitor had a maximal inhibitory efficacy of 96 percent at 400 mg/L. For a prospective corrosion inhibitor, the efficiency achieved is satisfactory [24]. The film created by WAC creates a barrier to the passage of electrons involved in redox processes, resulting in a change in the kinetics of the involved electrochemical processes [25].

3.1.3. Scanning electrochemical microscopy (SECM)

Scanning electrochemical microscopy is a ground-breaking method for detecting localized corrosion on metal surfaces. The methodology is capable of providing information on the electrochemical changes occurring on the surface, which may aid in the identification of an appropriate corrosion process. The SECM approach involves vibrating a probe near a metal surface and recording the produced current. The probe created more current when it was brought closer to the N80 steel surface, according to the approach. This might be owing to the probe's direct contact with the metal surface, which served as a conductor (Fig. 6a). Due to the insulating nature of the steel surface, a reduced current was measured when the same probe was brought nearer the steel surface with WAC inhibitor coating (Fig. 6b). As a result, the WAC inhibitor coating acts as an insulator, allowing the probe to detect lesser currents, but in the absence of the film, the steel acts as a conductor, causing the probe to record a greater current.

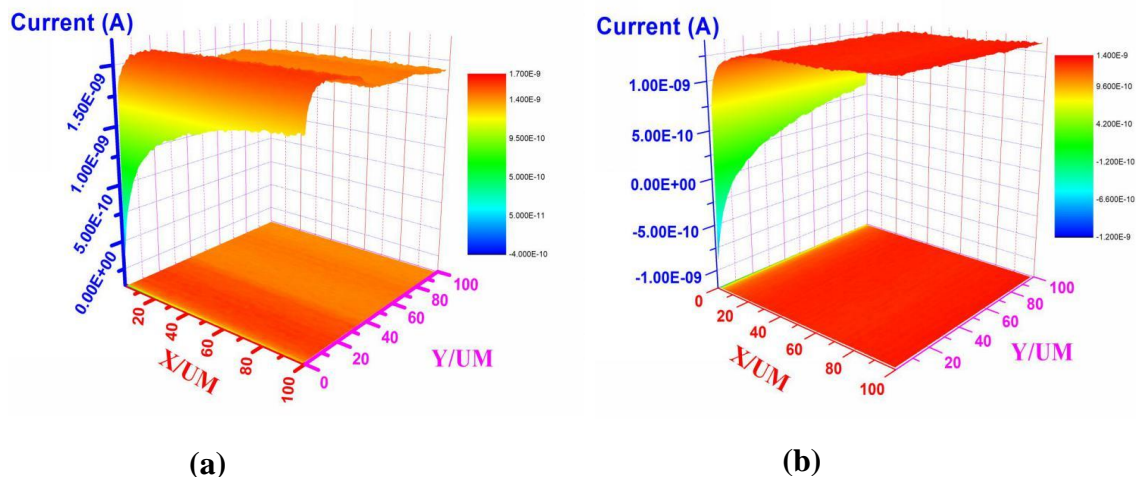
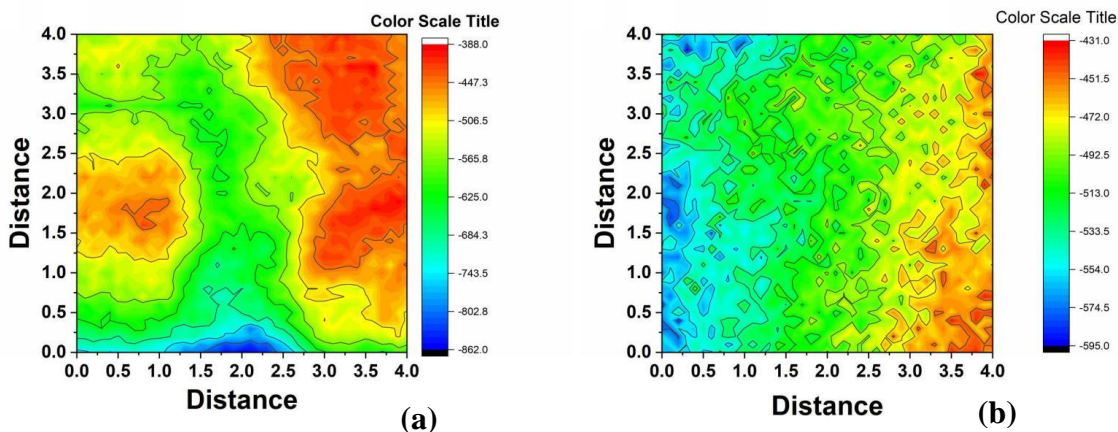


Figure 6. SECM 3D images of (a) blank + N80 steel and (b) inhibitor + N80 steel at a distance of 100 μm .

3.1.4. Scanning Kelvin Probe (SKP)

Although SKP is a useful approach, there is a scarcity of information on corrosion inhibitors. The probe vibrates across the metal surface, creating a current flow that acts as a capacitor. The voltage created at the electrode may be used to distinguish the anodic and cathodic zones. As illustrated in Fig. 7, the active anodic zones have a lower potential and the cathodic zone has a larger potential. There are 2D contour graphs and 3D graphs in the picture. As seen in Fig. 7a, 7c, the lower areas of anodic potential depict corrosion on the metal surface. The red and brown color patches on the steel surface are shown as anodic or corroded in the 2D contour and 3D figures [26]. The anodic zone on the steel coated with WAC inhibitor film is reduced (Fig. 7b, 7d). As a result, the presence of an inhibitor layer adsorbed on the steel surface decreases or inhibits anodic activity, reducing corrosion.



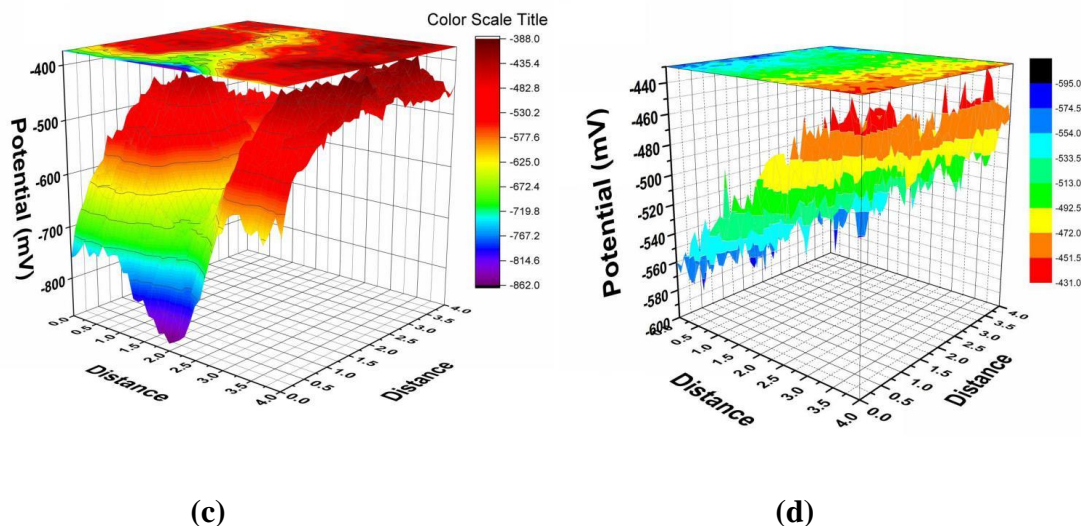


Figure 7. (a) Contour graph of blank + N80 steel (b) Contour graph for inhibitor + N80 steel (c) 3D colourmap image of blank + N80 steel (d) 3D colourmap image of inhibitor + N80 steel.

3.2. Surface analysis

3.2.1. Scanning electron microscopy (SEM)

The N80 steel was subjected to 400 mg/L WAC inhibitor and blank artificial saltwater. As illustrated in Fig. 8, the steel surface was cleaned, vacuum dried, and then exposed to the machine for surface studies. Without WAC in artificial saltwater, the surface of N80 steel looks rough, fractured, and rusted (Fig. 8a).

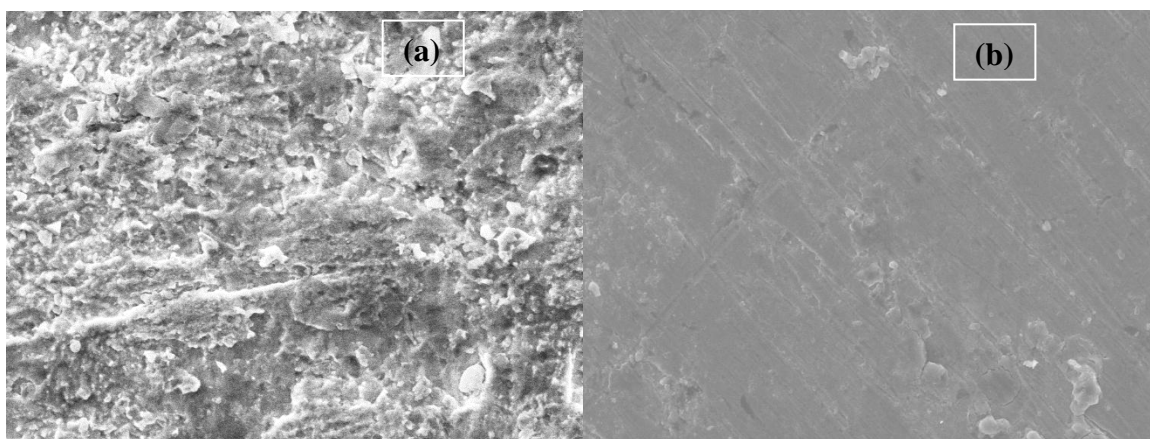


Figure 8. SEM micrographs of N80 steel in (a) in artificial seawater solution, and (b) inhibited solution.

This might be owing to the aggressive medium causing a hasty dissolving response at the electrode. Nonetheless, the N80 steel surface looked to be less corroded, undamaged, and smooth when it was coated with WAC in the same harsh medium (Fig. 8b). The lines were faintly evident

when the steel was abraded, and the mirror sheen was degraded by the action of artificial seawater [27].

4. CONCLUSIONS

1. In artificial seawater, a greater concentration of 400 mg/L WAC resulted in 96 percent inhibitor efficiency.

2. The impedance analysis also revealed that in the presence of WAC inhibitor, R_{ct} values are higher.

3. Polarization curve analysis revealed a prominent cathodic shift with $-E_{corr}$ values ranging between 80 mV.

4. SECM tests revealed a lower current in the presence of WAC and a larger current in the absence of WAC, but SKP revealed fewer anodic areas on the steel surface with WAC film.

5. SEM images of N80 steel with WAC layer and corroded without WAC inhibitor revealed a smooth surface.

ACKNOWLEDGEMENT

The authors are grateful to the Youth Scientific and Innovation Research Team for Advanced Surface Functional Materials, Southwest Petroleum University, 2018CXTD06.

References

1. Gavrilović Šekularac and Ingrid Milošević, *Corros. Sci.*, 144 (2018) 54.
2. Shiqiang Chen and Dun Zhang, *Corros. Sci.*, 148 (2019) 71.
3. A. Singh, K. Ansari, A. Kumar, W. Liu, C. Songsong and Y. Lin, *J. Alloy. Compd.*, 712 (2017) 121.
4. G. Quartarone, M. Battilana, L. Bonaldo and T. Tortato, *Corros. Sci.*, 50 (2008) 3467.
5. A. Singh, K. R. Ansari, D. S. Chauhan, M. A. Quraishi, H. Lgaz and I. M. Chung, *J. Coll. Inter. Sci.*, 560 (2020) 225.
6. Rouhollah Sabzi and Reza Arefinia, *Corros. Sci.*, 153 (2019) 292.
7. Hefang Wang, Meidan Gao, Yong Guo, Yongfang Yang and Rongbin Hu, *Desalination*, 398 (2016) 198.
8. Marwa Ben Harb, Samar Abubshait, Naceur Etteyeb, Madiha Kamoun and Adnene Dhouib, *Arab. J. Chem.*, 13 (2020) 4846.
9. M. A. Migahed, M. M. El-Rabiei, H. Nady and M. Fathy, *J. Environ. Chem. Eng.*, 4 (2016) 3741.
10. A. Singh, K.R. Ansari, J. Haque, P. Dohare, H. Lgaz, R. Salghi and M.A. Quraishi, *J. Taiwan Inst. Chem. E.*, 82 (2018) 233.
11. ASTM standard for Standard Practice for the Preparation of Substitute Ocean Water, Designation: D 1141 – 98 (Reapproved 2003), ASTM International, United States of America.
12. K.R. Ansari, M.A. Quraishi and Ambrish Singh, *Corros. Sci.*, 79 (2014) 5.
13. Ambrish Singh, Yuanhua Lin, K. R. Ansari, M. A. Quraishi, Eno. E. Ebenso, Songsong Chen and

- Wanying Liu, *Appl. Surf. Sci.*, 359 (2015) 331.
14. S. A. Haddadi, E. Alibakhshi, G. Bahlakeh, B. Ramezanzadeh and M. Mahdavian, *J. Mol. Liq.*, 284 (2019) 682.
 15. A. Singh, K.R. Ansari, A. Kumar, W. Liu, C. Songsong and Y. Lin, *J. Alloy Compd.*, 712 (2017) 121.
 16. K. Habib and K. Muhana, *Electrochem. Commun.*, 4 (2002) 54.
 17. M. Ramezanzadeh, Z. Sanaei, G. Bahlakeh and B. Ramezanzadeh, *J. Mol. Liq.*, 256 (2018) 67.
 18. Shougang Chen, Yan Chen, Yanhua Lei and Yansheng Yin, *Electrochem. Commun.*, 11(2009) 1675.
 19. S. Abrishami, R. Naderi and B. Ramezanzadeh, *Appl. Surf. Sci.*, 457 (2018) 487.
 20. K. R. Ansari, Dheeraj Singh Chauhan, M. A. Quraishi, Mohammad A. J. Mazumder and Ambrish Singh, *Int. J. Bio. Macro.*, 1441 (2020) 305.
 21. Qiongyu Zhou, Saad Sheikh, Ping Ou, Dongchu Chen and Sheng Guo, *Electrochem. Commun.*, 98 (2019) 63.
 22. Yang Yaocheng, Yin Caihong, Ambrish Singh and Yuanhua Lin, *New J. Chem.*, 43 (2019) 16058.
 23. A. Singh, K. R. Ansari, X. Xu, Z. Sun, A. Kumar and Y. Lin, *Sci. Rep.*, 7 (2017) 14904.
 24. Ambrish Singh, I Ahamad, V. K. Singh and M. A. Quraishi, *J. Sol. State Electrochem.*, 15 (2011) 1087.
 25. A. Singh, K.R. Ansari, M.A. Quraishi, H. Lgaz and Y. Lin, *J. Alloy Compd.*, 762 (2018) 347.
 26. A. Nazarov, M. G. Olivier and D. Thierry, *Prog. Org. Coat.*, 74 (2012) 356.
 27. K.R. Ansari, M.A. Quraishi and A. Singh, *Corros. Sci.*, 79 (2014) 5.

© 2021 The Authors. Published by ESG (www.electrochemsci.org). This article is an open access article distributed under the terms and conditions of the Creative Commons Attribution license (<http://creativecommons.org/licenses/by/4.0/>).